Front. Earth Sci. 2023, 17(1): 109−120
https://doi.org/10.1007/s11707-022-1016-z

RESEARCH ARTICLE

Multi-stage gas diffusion and its implications for the productivity of coalbed methane in the southern Qinshui Basin, north China

Hui WANG[1,2], Yanbin YAO (✉)[1,2], Zhentao LI[3], Yanhui YANG[4], Junjie YI[5], Yongkai QIU[1,2], Shengqiang ZHOU[1,2]

1 School of Energy Resource, China University of Geosciences, Beijing 100083, China
2 Coal Reservoir Laboratory of National Engineering Research Center of CBM Development & Utilization, China University of Geosciences, Beijing 100083, China
3 State Key Laboratory of Organic Geochemistry, Guangzhou Institute of Geochemistry, Chinese Academy of Sciences, Guangzhou 510640, China
4 PetroChina Huabei Oilfield Company, Renqiu 062552, China
5 Institute of Mineral Resources Research, Beijing 101300, China

Abstract The behavior of coalbed methane (CBM) diffusion considerably influences gas productivity. Based on the multi-porous diffusion model and on-site CBM desorption data of coal cores, the behavior of CBM diffusion and its implications on the gas productivity of No. 3 coal seam in the southern Qinshui Basin (SQB) were elaborately analyzed. Results indicate that CBM diffusion of No. 3 coal seam demonstrates noticeable three-stage characteristics, including the fast diffusion, transitional diffusion, and slow diffusion stages. During the gas diffusion process, the gas content and/or the degree of developed pores and fractures/cleats in coal seams can affect the desorption of CBM and the amount of diffused CBM by influencing the changes in gas pressure in pores, thus controlling the behavior of gas diffusion in different stages. Because gas content and the developed degree of pores and fractures/cleats are closely associated with the deformation degree of the coal seams, variably deformed coal seams exhibit unique characteristics of gas diffusion. The low-deformation degree of the coal seams have a relatively uniform distribution of gas production over the history of a well. By contrast, the moderate-deformation degree of the coal seams have a relatively high rate and amount of gas diffusion in the fast and transitional diffusion stages, producing most of the gas in the early-to-intermediate stages of the wells. Finally, the high-deformation degree of the coal seams has a high rate and amount in the fast diffusion stage, indicating that most of the production stage occurs during the early stage of the gas production history of a well. In summary, the behavior of gas diffusion can be used for predicting gas production potential.

Keywords coalbed methane, gas diffusion, CBM production, coal deformation, Qinshui Basin

Received February 11, 2022; accepted June 6, 2022

E-mail: yyb@cugb.edu.cn

1 Introduction

Coalbed methane (CBM), an abundant clean fuel with a considerable long-term development potential (Karacan et al., 2011; Pillalamarry et al., 2011; Moore, 2012), is an important source of gas supply for many countries, such as the Unites States, Australia, and China. In China, thousands of CBM production wells have been drilled in the southern Qinshui Basin (SQB), providing the highest contribution to China's total output of CBM. Within the SQB, the Zhengzhuang Field is well-developed and the Anze–Mabi Fields are in early development stage, with a total area of approximately 3000 km^2 (Fig. 1). Although CBM enrichment mechanisms (Cai et al., 2011; Zhang et al., 2018; Liu et al., 2022a) have been studied by many researchers in these fields, the high heterogeneity in reservoir productivity is not well understood.

CBM production is a complex process, comprising three phases of gas movement: 1) desorption through the matrix, 2) diffusion into the fractures/cleats network and 3) flow through the fracture/cleat network to the wellbore (Ziarani et al., 2011; Keshavarz et al., 2017). Because

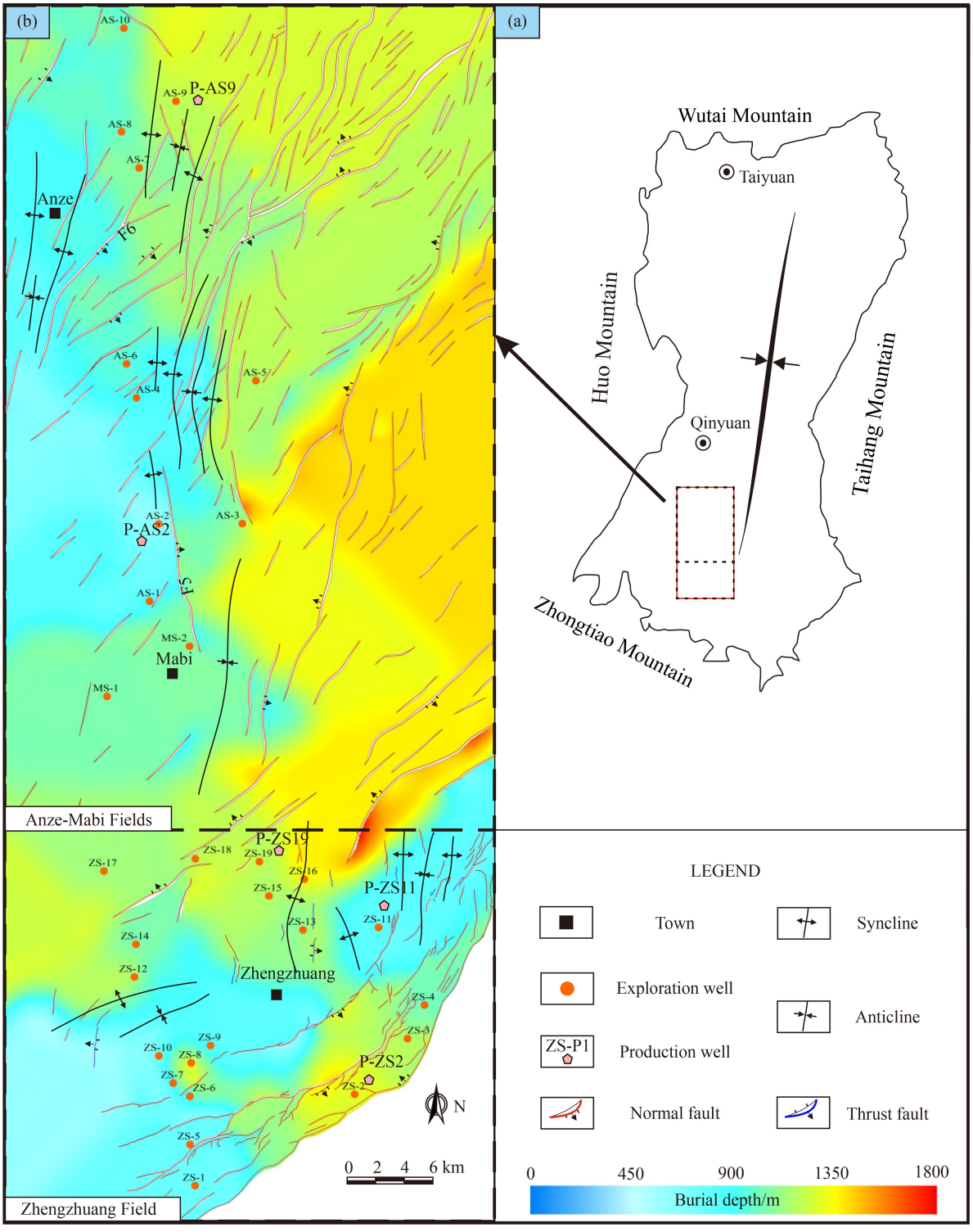

Fig. 1 (a) Location of the SQB in Qinshui Basin and (b) Geological structures and exploration wells locations, and the background shows a burial depth of the No. 3 coal seam in the SQB.

CBM diffusion refers to a gas exchange between the fracture/cleat and matrix of coals, its influence on reservoir productivity has attracted increasing interest (Pillalamarry et al., 2011; Ziarani et al., 2011; Staib et al., 2015; Li et al., 2021). The behavior of CBM diffusion significantly affects reservoir productivity (Pillalamarry et al., 2011; Ziarani et al., 2011; Li et al., 2021); however, there is no consensus on which stage of the production process (such as the early production and later production stages) it mainly affects. For example, using experimental

data modeling, Pillalamarry et al. (2011) showed that the CBM diffusivity rate considerably affected the production rate in the later production stage of gas production history. By contrast, Ziarani et al. (2011) suggested that the reservoir with a faster CBM diffusion behavior is conducive to more gas for early production. Therefore, the effect of CBM diffusion behavior on the productivity of each specific development area should be investigated.

CBM diffusion behavior is affected by several factors, including underground temperature–pressure conditions (Charrière et al., 2010; Tang et al., 2015) and the physical properties of the reservoir. For the physical properties of the reservoir, pore–fracture/cleat development (Lu et al., 2015; Cheng and Pan, 2020; Jia et al., 2021; Liu et al., 2022b), coal rank (Xu et al., 2015; Keshavarz et al., 2017), gas content (Li et al., 2021) and moisture content (Clarkson and Bustin, 1999; Pan et al., 2015) most closely correlate to CBM diffusion. Employing experimental measurements and numerical simulation, Keshavarz et al. (2017) found that the CBM diffusivity rate varied over six orders of magnitude for bituminous and subbituminous coals. Dong et al. (2020) found that deformed coals having unique pore–fracture/cleat systems can considerably affect CBM diffusion. Liu et al. (2020) found that the "scale-effect" of coal particles has a distinct influence on CBM diffusion. In a coal reservoir, a combined effect of multiple factors controls CBM diffusion behavior, which has not yet been investigated for the SQB, particularly in the developing fields (e.g., Anze–Mabi Fields). Some studies conducted in the developed fields performed isothermal adsorption/desorption experiments on coal samples collected from underground coal mines and/or field outcrops in the SQB (Meng and Li, 2016; Zhao et al., 2018) and these data cannot directly replicate the on-site behavior of CBM diffusion. This causes deviations from reservoir productivity estimates based on CBM diffusion. Therefore, on-site CBM desorption data for exploring the behavior of CBM diffusion and its influence on the gas production history of the wells in the SQB should be used.

Researchers have recently discovered that CBM diffusion behavior in coals tends to be multi-stage (Staib et al., 2015; Li et al., 2016; Yang et al., 2019). Li et al. (2016) proposed a multi-porous model for describing CBM diffusion, which was validated by experimental data. In this study, the CBM diffusion behavior was investigated using the combination of on-site CBM desorption data from coal cores and the multi-porous diffusion model proposed by Li et al. (2016). Then, the regional distribution of CBM diffusion properties and geological controls in the SQB were discussed. This study reported the results for the regional distribution of CBM diffusion behavior in the SQB and discusses its controlling factors. Finally, the effects of CBM diffusion behavior on gas productivity in the SQB were determined.

2 Geological setting

2.1 Tectonic setting

The Qinshui Basin is located in north China. The general tectonic appearance of the basin shows a large bilateral symmetric synclinorium with an NNE–SSW strike (Fig. 1(a)). It is structurally surrounded by four mountains, namely, Zhongtiao Mountain, Huo Mountain, Wutai Mountain, and Taihang Mountain (Fig. 1(a)). Since the Permo-Carboniferous period, four multi-stage tectonic activities have occurred in this basin, including the Indosinian Orogeny with SN-trending principal compressive stress, the Yanshanian Orogeny with NW-trending principal compressive stress, the Early Himalayan Orogeny with NWW-trending extensional stress and the Late Himalayan Orogeny with NNE-trending principal compressive stress (Cai et al., 2011). In the SQB, well-developed NE-trending normal faults (Fig. 1(b)) formed under NWW-trending extensional stress in the Early Himalayan Orogeny (Wang et al., 2016) and N–S-trending and NW–SE-trending folds (Fig. 1(b)) formed under NWW-trending extensional stress in the Jurassic–Cretaceous Yanshanian Orogeny (Cai et al., 2011).

2.2 Coal-bearing strata

In the SQB, the sedimentary strata dip at 3° to 13°, in which the Upper Pennsylvanian Taiyuan Formation (C_3t) and the Lower Permian Shanxi Formation (P_1s) are the primary coal-bearing strata (Fig. 2). The No. 3 coal seam in the Shanxi Formation mainly comprises anthracite coal with lesser amounts of bituminous coal, corresponding to the maximum vitrinite reflectance ($R_{o,m}$) of 1.8%–4.3%. The deformation extent of the No. 3 coal seam varies from high to low in the SQB (Wang et al., 2022). Moreover, it typically has a thickness of 2–8 m (avg. = 6.0 m), burial depth of 300–1500 m (see the background of Fig. 1(c)), and gas content of 8.9–30.5 m^3/t (avg. = 19.9 m^3/t). The details of some primary properties of the No.3 coal seam are listed in Table 1. This study selects the No. 3 coal seam as representative for investigating the CBM diffusion behavior and its influence on reservoir productivity in the SQB.

3 Data and methods

3.1 Data source

All data used in this study, including the on-site CBM desorption data, gas content, and well production history, were provided by PetroChina Huabei Oilfield Company. In this study, the desorption data of coal cores from 31 CBM exploration wells (Fig. 1) were used, and these data

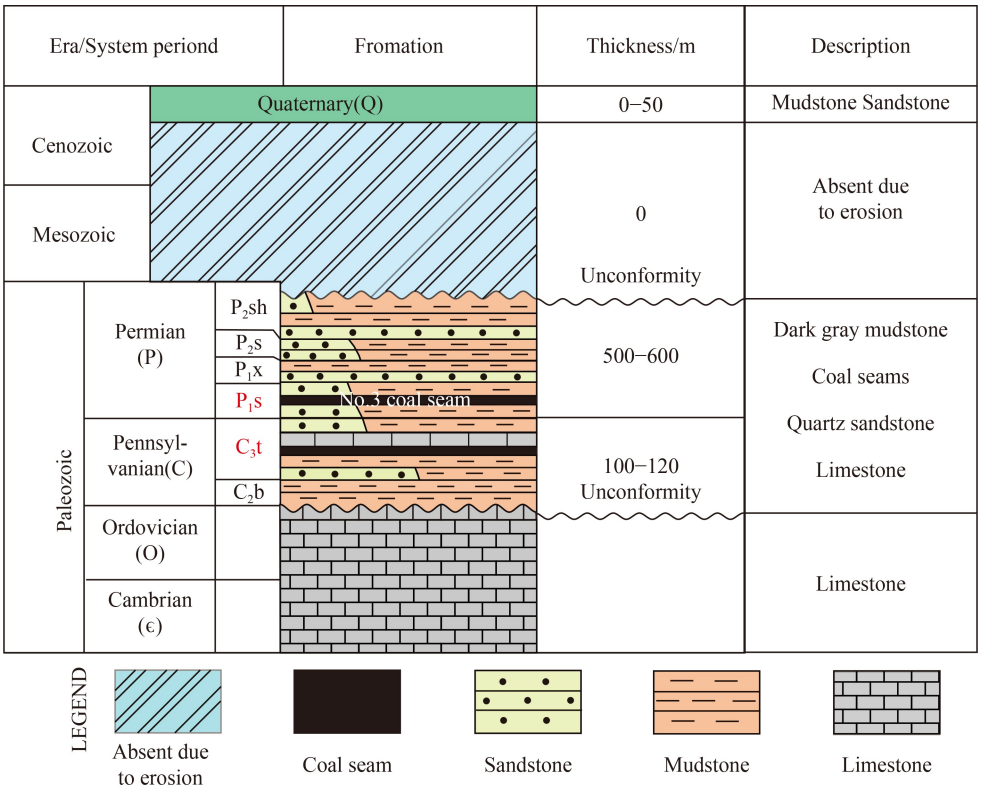

Fig. 2 Stratigraphic column in the SQB.

Table 1 The primary properties of No. 3 coal seam in the SQB (well locations can be found in Fig. 1)

Well	Coal seam deformation degree	V_d /(m^3·t^{-1})	V_t /(m^3·t^{-1})	Well	Coal seam deformation degree	V_d /(m^3·t^{-1})	V_t /(m^3·t^{-1})
ZS-1	M	18.3	19.9	ZS-17	L	27.1	30.5
ZS-2	M	22.4	23.9	ZS-18	M	27.8	30
ZS-3	L	19.4	21.5	ZS-19	L	21.3	23.4
ZS-4	L	24.2	27.1	MS-2	H	14.1	15.3
ZS-5	L	20.8	23.2	MS-3	M	20.5	22.5
ZS-6	L	20.8	21.8	AS-1	H	9.0	9.9
ZS-7	L	21.0	22.3	AS-2	M	9.8	13.2
ZS-8	M	8.1	12.6	AS-3	L	23.0	25.3
ZS-9	L	17.3	17.7	AS-4	H	12.0	13
ZS-10	L	20.0	21.4	AS-5	L	15.1	16.8
ZS-11	H	17.2	18.2	AS-6	H	10.0	11.4
ZS-12	L	24.3	27.8	AS-7	H	9.8	10.7
ZS-13	L	24.9	27.8	AS-8	M	18.4	21.2
ZS-14	L	19.1	20.4	AS-9	H	0.9	8.9
ZS-15	L	23.9	25.4	AS-10	H	9.4	10.4
ZS-16	L	18.9	21.2	–	–	–	–

Notes: L = Low-deformation degree of the coal seam; M = Moderate-deformation degree of the coal seam; H = High-deformation degree of the coal seam; V_d = Desorbed gas content of the coal seam; V_t = Total gas content of the coal seam.

were measured by the on-site test followed the Chinese standard GB/T 19559-2008. A detailed descriptions of this test can also be found in the studies by Li et al. (2020) and Li et al. (2021). Specifically, the airtight detection was first conducted for the desorption canister and metering unit before tests. And then, the tests were performed under the similar atmospheric pressure (~0.1 MPa) and temperature conditions (~25°C). For a coal core, the on-site desorption test was conducted when the desorption volume was less than 10 cm^3/d for seven

consecutive days. Then, the coal core was sent to the laboratory and crushed into fragments (2–3 cm and 300–500 g) for residual gas measurement that was used for calculating the total gas content. The residual gas measurement adopted the same method as the on-site desorption test. Furthermore, the production history data were collected from five typical wells that had been produced over 600 days. Detailed sampling information and the aforementioned data results are presented in Table 1.

3.2 Modeling of CBM diffusion process

Using the isothermal adsorption data of coals, Li et al. (2016) proposed a multi-porous diffusion model for determining the diffusion parameters of different stages. Based on this multi-porous diffusion model, Li et al. (2021) divided the CBM diffusion process into the fast diffusion stage, the transitional diffusion stage and the slow diffusion stage of coal seams in the northern Qinshui Basin. This result was introduced to the SQB in this study. The following equations represent these three stages:

$$\frac{M_a}{M_{a\infty}} = 1 - \frac{6}{\pi^2}\sum_{n=1}^{\infty}\frac{1}{n^2}\exp\left(-D_1 n^2\pi^2 t\right), \quad (1)$$

$$\frac{M_b}{M_{b\infty}} = 1 - \frac{6}{\pi^2}\sum_{n=1}^{\infty}\frac{1}{n^2}\exp\left(-D_2 n^2\pi^2 t\right), \quad (2)$$

$$\frac{M_c}{M_{c\infty}} = 1 - \frac{6}{\pi^2}\sum_{n=1}^{\infty}\frac{1}{n^2}\exp\left(-D_3 n^2\pi^2 t\right), \quad (3)$$

$$\frac{M_t}{M_{\infty}} = \beta_1\frac{M_a}{M_{a\infty}} + \beta_2\frac{M_b}{M_{b\infty}} + \beta_3\frac{M_c}{M_{c\infty}}, \quad (4)$$

where M_a, M_b, M_c, M_t, and $M_{i\infty}$, represent the amount of gas desorbed from the fast diffusion stage, the transitional diffusion stage, the slow diffusion stage, the amount of gas desorption at time t and the total amount of gas desorbed from i-th stage at an indefinite time, respectively; D_1, D_2, and D_3 represent the effective diffusion coefficients of the fast diffusion stage, the transitional diffusion stage and the slow diffusion stage, respectively and β_1, β_2, and β_3, are the ratios of the fast diffusion stage, the transitional diffusion stage and the slow diffusion stage, respectively ($\beta_1 + \beta_2 + \beta_3 = 1$).

4 Results and discussion

4.1 Calculation of CBM diffusion coefficients and proportions

The diffusion coefficients and proportions of different diffusion stages were obtained by transforming the multi-porous diffusion model (Eqs. (1)–(4)) into a fitting program (Python code) and appropriately setting the number of iterations and the initial values. Table 2 lists the fitting results of on-site CBM desorption data through the multi-porous diffusion model, and some representative fitting results are shown in Fig. 3. As shown, the fitting results demonstrate that the values of the fast diffusion coefficient (D_1), the transitional diffusion coefficient (D_2) and the slow diffusion coefficient (D_3) of the No. 3 coal seam in the SQB all cover three orders of magnitude. Furthermore, the values of the proportion of fast diffusion stage (β_1), the proportion of transitional diffusion stage (β_2) and the proportion of slow diffusion stage (β_3) are 0.32–0.73, 0.15–0.42, and 0.09–0.30, respectively.

4.2 CBM diffusion characteristics and regional distribution in the SQB

4.2.1 Fast diffusion stage

By plotting the fitting results into contour maps, the regional distributions of the proportion of diffusion stages (β_1, β_2, and β_3, see Fig. 4) and diffusion coefficients (D_1, D_2, and D_3, see Fig. 5) were analyzed. Results show that the relatively low proportion of the fast diffusion stage ($0.26 < \beta_1 < 0.48$, avg. = 0.38) and low fast diffusion coefficient (1.05×10^{-3} h^{-1} $< D_1 < 1.32 \times 10^{-2}$ h^{-1}, avg. = 5.09×10^{-3} h^{-1}) are mainly west of Zhengzhuang town and east of Mabi town (Figs. 4 and 5(a)), where coal seams have a low-deformation degree (see background of Fig. 4). Table 1 shows that the low-deformation coal seams have a high gas content of 16.8–30.5 m^3/t (avg. = 23.4 m^3/t). However, the proportion and coefficient of the fast diffusion stage are generally low in the low-deformation degree of the coal seams (Figs. 6(a) and 6(b)). This result suggests that the low proportion of CBM diffusion in the fast diffusion stage is probably resulted from the poor development of pores and fractures/cleats in the low-deformation degree of the coal seams (Cheng and Pan, 2020; Wang et al., 2022).

As shown in Figs. 4 and 5, the relatively high proportion of the fast diffusion stage ($0.41 < \beta_1 < 0.72$, avg. = 0.55) and high fast diffusion coefficient (3.35×10^{-3} h^{-1} $< D_1 < 1.58 \times 10^{-2}$ h^{-1}, avg. 9.64×10^{-3} h^{-1}) are mainly east of Zhengzhuang town where moderate-deformation degree of the coal seams are well-developed. Furthermore, the high-deformation degree of the coal seams have a high proportion of the fast diffusion stage ($0.57 < \beta_1 < 0.73$, avg. = 0.67) and low fast diffusion coefficient ($D_1 < 5.72 \times 10^{-3}$ h^{-1}) in the Anze–Mabi Fields. With regard to the moderate and high-deformation degree of the coal seams, the fast diffusion coefficient is generally low ($D_1 < 6.0 \times 10^{-3}$ h^{-1}) when gas content is less than 15 m^3/t (Fig. 6(b)). In terms of relatively high gas content (> 15 m^3/t), the fast diffusion coefficient has

Table 2 CBM diffusion parameters of 31 coal cores from No. 3 coal seam of the SQB based on the multi-porous diffusion model

Well	β_1	$D_1/(h^{-1})$	$V_1/(m^3 \cdot t^{-1})$	β_2	$D_2/(h^{-1})$	$V_2/(m^3 \cdot t^{-1})$	β_3	$D_3/(h^{-1})$	$V_3/(m^3 \cdot t^{-1})$
ZS-1	0.57	1.06×10^{-2}	10.4	0.31	1.52×10^{-3}	5.7	0.12	4.70×10^{-4}	2.2
ZS-2	0.57	1.45×10^{-2}	12.8	0.33	1.73×10^{-3}	7.4	0.10	5.35×10^{-4}	2.2
ZS-3	0.35	1.32×10^{-2}	6.8	0.37	1.83×10^{-3}	7.2	0.28	8.50×10^{-4}	5.4
ZS-4	0.39	8.85×10^{-3}	9.4	0.35	1.45×10^{-3}	8.5	0.27	7.33×10^{-4}	6.5
ZS-5	0.33	7.96×10^{-3}	6.9	0.38	1.85×10^{-3}	7.9	0.29	7.20×10^{-4}	6.0
ZS-6	0.36	5.68×10^{-3}	7.5	0.38	1.46×10^{-3}	7.9	0.26	4.35×10^{-4}	5.4
ZS-7	0.37	5.85×10^{-3}	7.8	0.35	1.62×10^{-3}	7.4	0.28	6.28×10^{-4}	5.9
ZS-8	0.41	9.30×10^{-3}	8.2	0.42	1.30×10^{-3}	8.4	0.17	5.50×10^{-4}	3.4
ZS-9	0.38	4.15×10^{-3}	3.1	0.34	1.85×10^{-3}	2.8	0.28	6.60×10^{-4}	2.3
ZS-10	0.32	4.83×10^{-3}	5.5	0.42	2.05×10^{-3}	7.3	0.26	7.10×10^{-4}	4.5
ZS-11	0.56	1.58×10^{-2}	11.4	0.33	6.91×10^{-4}	6.7	0.11	2.10×10^{-4}	2.2
ZS-12	0.44	4.03×10^{-3}	10.7	0.31	2.40×10^{-3}	7.5	0.25	6.10×10^{-4}	6.1
ZS-13	0.42	5.76×10^{-3}	10.5	0.38	1.98×10^{-3}	9.5	0.20	6.58×10^{-4}	5.0
ZS-14	0.33	4.53×10^{-3}	6.3	0.39	2.15×10^{-3}	7.4	0.28	7.08×10^{-4}	5.3
ZS-15	0.47	5.53×10^{-3}	11.2	0.29	1.82×10^{-3}	6.9	0.24	5.73×10^{-4}	5.7
ZS-16	0.35	3.46×10^{-3}	6.6	0.38	1.85×10^{-3}	7.2	0.27	4.22×10^{-4}	5.1
ZS-17	0.38	1.95×10^{-3}	10.3	0.39	1.60×10^{-3}	10.6	0.23	5.10×10^{-4}	6.2
ZS-18	0.46	8.21×10^{-3}	12.8	0.37	2.30×10^{-3}	10.3	0.17	4.40×10^{-4}	4.7
ZS-19	0.33	6.50×10^{-3}	7.0	0.37	2.00×10^{-3}	7.9	0.30	8.20×10^{-4}	6.4
MS-2	0.72	5.72×10^{-3}	10.2	0.15	4.59×10^{-4}	2.1	0.13	2.20×10^{-4}	1.8
MS-3	0.56	3.35×10^{-3}	11.5	0.27	6.20×10^{-4}	5.5	0.17	3.70×10^{-4}	3.5
AS-1	0.66	5.48×10^{-3}	5.9	0.20	4.23×10^{-4}	1.8	0.14	1.35×10^{-4}	1.3
AS-2	0.60	3.88×10^{-3}	5.9	0.24	1.80×10^{-3}	2.4	0.16	6.00×10^{-4}	1.6
AS-3	0.41	1.28×10^{-3}	9.4	0.31	2.05×10^{-3}	7.1	0.28	7.80×10^{-4}	6.4
AS-4	0.71	5.30×10^{-3}	8.5	0.19	5.13×10^{-4}	2.3	0.10	2.00×10^{-4}	1.2
AS-5	0.48	1.05×10^{-3}	7.2	0.34	7.07×10^{-4}	5.1	0.18	5.10×10^{-4}	2.7
AS-6	0.73	5.01×10^{-3}	7.3	0.18	6.63×10^{-4}	1.8	0.09	1.60×10^{-4}	0.9
AS-7	0.70	5.56×10^{-3}	6.9	0.19	6.23×10^{-4}	1.9	0.11	1.70×10^{-4}	1.1
AS-8	0.57	2.21×10^{-3}	10.5	0.25	1.35×10^{-3}	4.6	0.18	5.18×10^{-4}	3.3
AS-9	0.68	5.19×10^{-3}	0.6	0.18	6.50×10^{-4}	0.2	0.14	1.40×10^{-4}	0.1
AS-10	0.72	5.38×10^{-3}	6.8	0.15	6.15×10^{-4}	1.4	0.13	1.36×10^{-4}	1.2

Notes: D_1, D_2, and D_3 represent the CBM diffusion coefficient of the fast, transitional and slow diffusion stages. β_1, β_2, and β_3 are the proportion of the fast, transitional and slow diffusion stages, and $\beta_1 + \beta_2 + \beta_3 = 1$. V_1, V_2, and V_3 are the absolute amount of diffused CBM in the fast, transitional and slow diffusion stages ($V_i = \beta_i \times V_d$, i = 1, 2, and 3, V_d can be seen in Table 1).

an increasing trend with increasing gas content (Fig. 6(b)). Because the moderate and high-deformation degrees of the coal seams commonly have well-developed pore–fracture/cleats (Cheng and Pan, 2020; Wang et al., 2022), it seems that the gas content in these seams controls CBM diffusion in the fast diffusion stage.

4.2.2 Transitional diffusion stage

Figures 4 and 5(b) show a high transitional diffusion proportion ($\beta_2 > 0.29$) and a high transitional diffusion coefficient ($D_2 > 7.07 \times 10^{-4}$ h^{-1}) in the regions where the low-deformation degree of the coal seams are well-developed (such as west of Zhengzhuang town). In the regions with good development of the moderate-deformation degree of the coal seams, the transitional diffusion proportion is generally high (> 0.31) and the transitional diffusion coefficient ranges from 6.20×10^{-4} h^{-1} to 2.30×10^{-3} h^{-1} (avg. = 1.52×10^{-3} h^{-1}, see Table 2). There is a relatively low transitional diffusion proportion (β_2) of 0.15–0.33 (avg. = 0.19) and transitional diffusion coefficient (D_2) of < 6.63×10^{-4} h^{-1} in the regions with a well-developed high-deformation degree of the coal seams. These results mean that the rate of

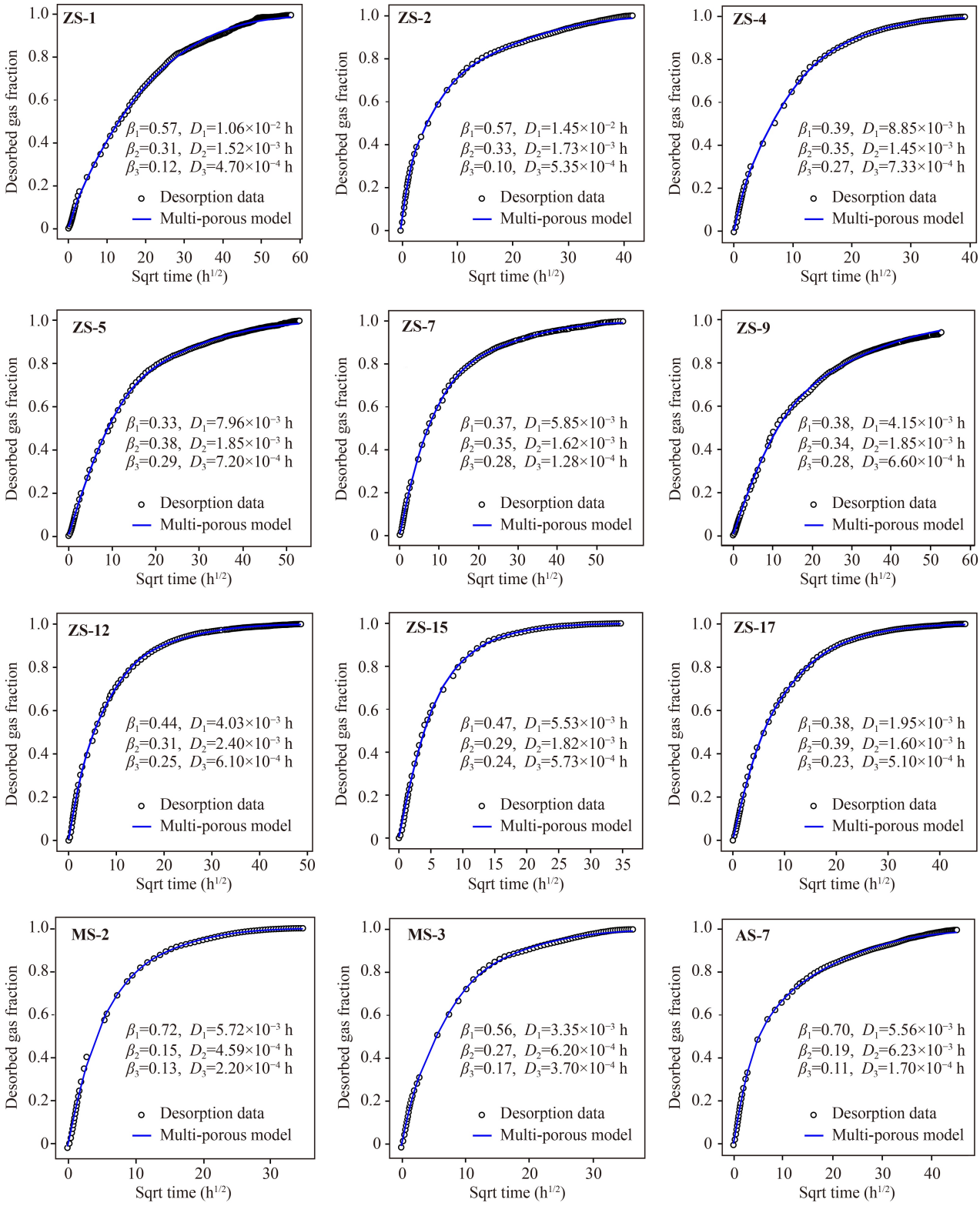

Fig. 3 Fitting results of the on-site CBM desorption data of representative wells in the SQB. The behavior of CBM diffusion can be well represented by the multi-porous diffusion model (Eqs. (1) to (4)) and demonstrates obvious three-stage characteristics.

CBM diffusivity in the high-deformation degree of the coal seams is greatly reduced (approximately 7 to 23 times, avg. 11 times) after the fast diffusion stage, followed by the moderate-deformation coal seams with a reduction of approximately 2–8 times (avg. = 5 times) and the low-deformation degree of the coal seam with a reduction of approximately 1–7 times (avg. = 3 times). As shown in Fig. 6(c), there is a positive relationship be-

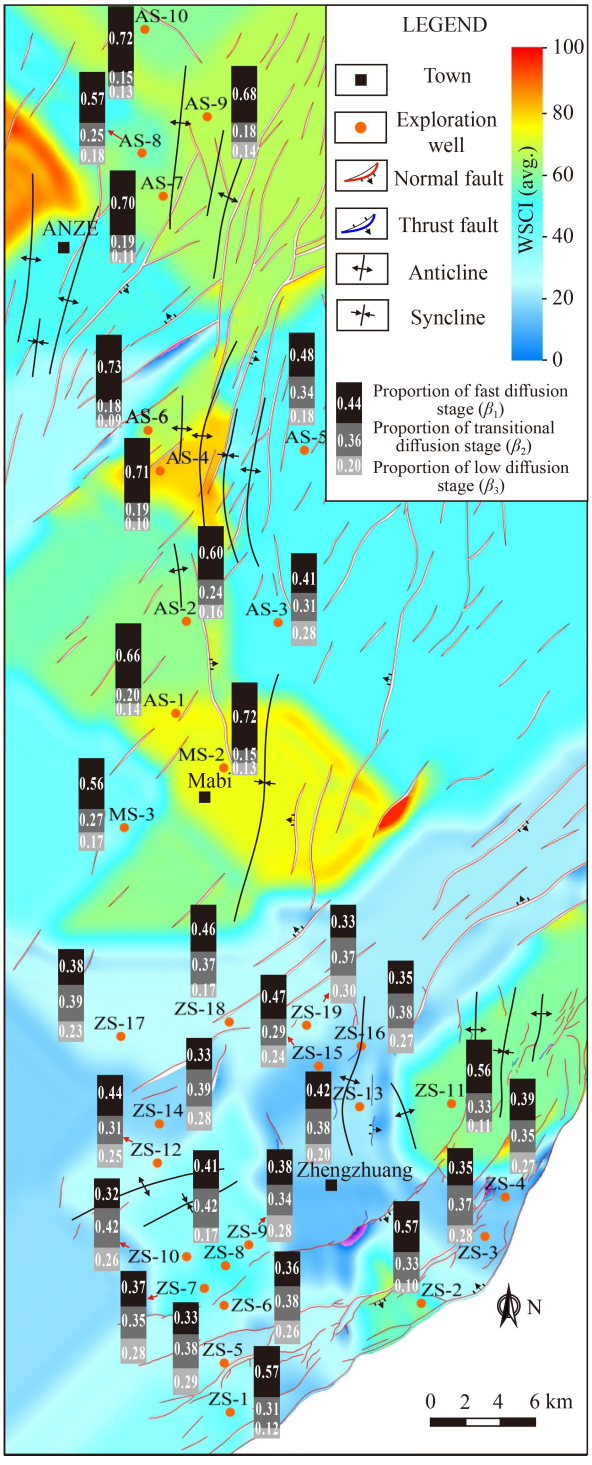

Fig. 4 The regional distribution of WCSI (avg.) of the No. 3 coal seam in the SQB with some wells added the proportion of fast, transitional and slow diffusion stages. The background of this figure is referenced from the previous studies by Wang et al. (2022), in which the deformation degree of the coal seams can be divided into low (WCSI (avg.) < 40), moderate (40 < WCSI (avg.) < 60) and high (WCSI (avg.) > 60) by a parameter of WCSI (avg.).

tween gas content and the proportion of the transitional diffusion stage. This result suggests that high gas content contributes to a high proportion of transitional diffusion stage in any coal seam. In addition, the transitional diffusion coefficient is relatively homogeneous in similar deformation degree coal seams (Fig. 6(d)), reflecting control of the development of pores and fractures/cleats in coal seams.

4.2.3 Slow diffusion stage

Figures 4 and 5(c) show relatively high slow diffusion proportion ($0.18 < \beta_3 < 0.30$, avg. = 0.26) and slow diffusion coefficient ($D_3 > 4.22 \times 10^{-4}$ h^{-1}) in the regions where low-deformation coal seams are well-developed (such as north of the Zhengzhuang town). In the regions with well-developed moderate deformation coal seams (such as the east of the Zhengzhuang town, south of Anze town, and west of the Mabi town), the slow diffusion proportion ranges from 0.10 to 0.18 (avg. = 0.15) and slow diffusion coefficient ranges from 3.70×10^{-4} h^{-1} to 6.00×10^{-4} h^{-1} (avg. = 4.97×10^{-4} h^{-1}, see Table 2). Figures 4 and 5(c) show that the regions with a high-deformation degree of the coal seams present a low slow diffusion proportion (β_3) of 0.09–0.14 (avg. = 0.12) and slow diffusion coefficient (D_3) of 1.35–2.20 $\times 10^{-4}$ h^{-1} (Table 2). These results indicate that the rate of CBM diffusivity in the high-deformation degree of the coal seams is greatly reduced (approximately 3.5 times) after the transitional diffusion stage, which is followed by the moderate-deformation degree of the coal seam with a reduction of approximately 3.0 times and the low-deformation coal seams with a reduction of approximately 2.8 times. Figure 6(e) shows that the proportion of the slow diffusion stage (β_3) has a positive correlation to gas content. In addition, the slow diffusion coefficient from high to low corresponds to low deformation, followed by the moderate deformation and high deformation degree of the coal seams (Fig. 6(f)). This reflects that the behavior of slow diffusion is mainly influenced by a combination of pore–fracture/cleat development and gas content in coal seams.

4.3 Amount of CBM diffuses in different stages

In general, the CBM in a coal reservoir comprises the dominating adsorption gas (Liu et al., 2022c), a few free gases, and negligible water-soluble gases. Thus, most diffused CBM has to be first desorbed from the surface of the coal matrix, a process which is very sensitive to reservoir pressure (Clarkson and Salmachi, 2017). This means that the changes in reservoir pressure can affect CBM desorption and the amount of diffused CBM.

With regard to the low-deformation degree of the coal seam, the large amount of CBM is probably desorbed with a sudden drop of reservoir pressure in the initial fast diffusion stage. However, the desorbed CBM cannot diffuse quickly from the matrix to pore–fracture/cleat

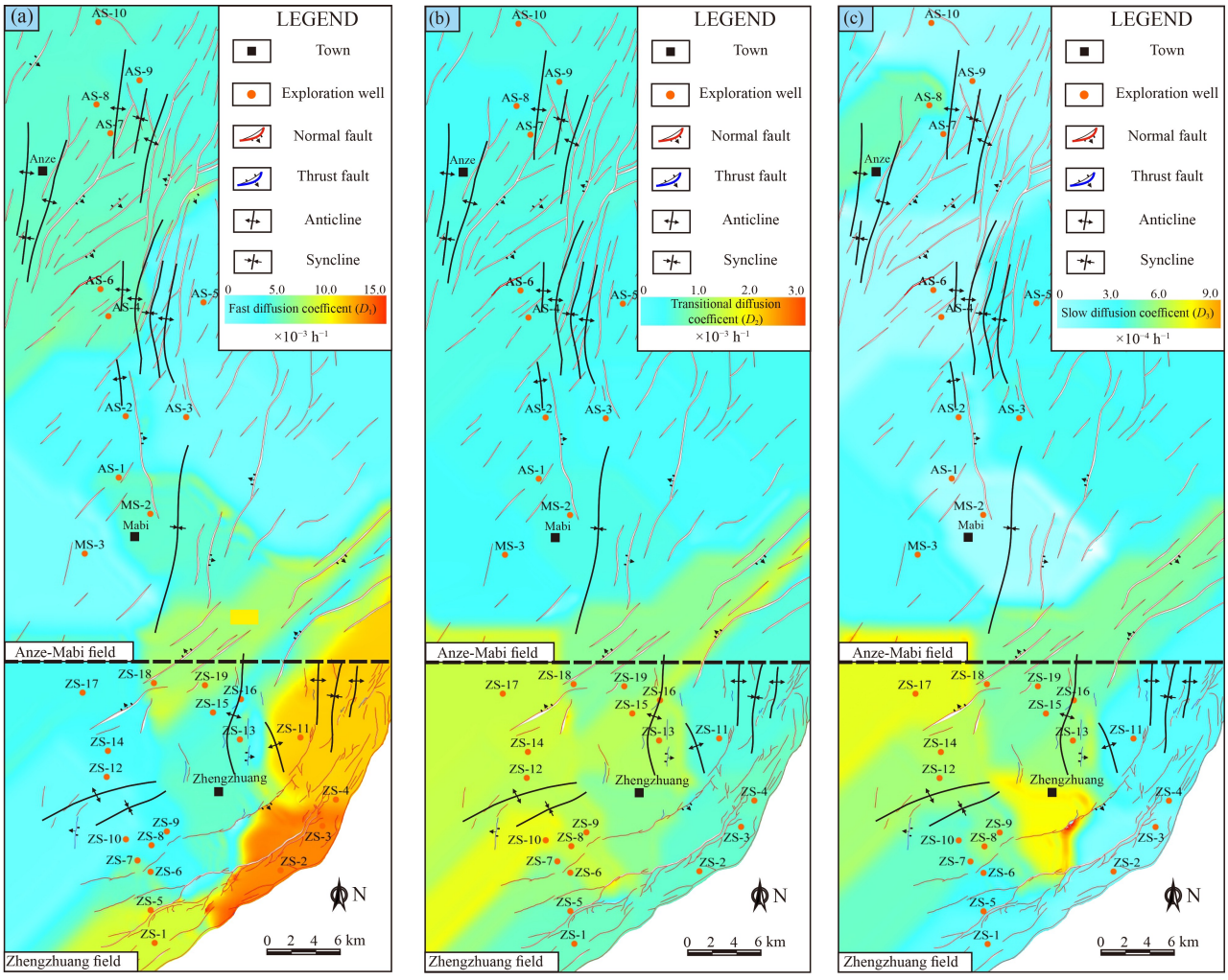

Fig. 5 Contour map of the fast diffusion coefficient (a), the transitional diffusion coefficient (b) and the slow diffusion coefficient (c) of No. 3 coal seam in the SQB.

networks (Fig. 6(b)) because of poor development of pores and fractures/cleats in the coal seams. This can result in an increase in gas pressure in pores, which affects the CBM diffusivity rate in the fast diffusion stage. After the fast diffusion stage, the remaining CBM content is relatively high, thus large gas volumes can desorb in both the transitional and slow diffusion stages. This results in a relatively homogeneous distribution of the amount of CBM diffusion in the fast diffusion stage (3.1–11.2 m^3/t, avg. = 7.9 m^3/t), the transitional diffusion stage (2.8–10.6 m^3/t, avg. = 7.4 m^3/t) and the slow diffusion stage (2.3–6.5 m^3/t, avg. = 5.3 m^3/t), as shown in Table 2.

For the moderate-deformation degree of the coal seam, the amount of desorbed CBM is relatively high with a sudden drop of reservoir pressure in the fast diffusion stage and the desorbed CBM can diffuse quickly through the developed pores and fractures/cleats in the coal seam. This is favorable for continuous gases desorption and contributes to the relatively high CBM diffusivity rate in the fast diffusion stage (Fig. 6(b)). Table 2 shows that the amount of CBM diffused in the fast diffusion stage (5.9–12.8 m^3/t, avg. = 10.3 m^3/t) and transitional diffusion stage (2.4–10.3 m^3/t, avg. = 6.3 m^3/t) represents approximately 80% of the total amount for the moderate-deformation degree coal seams. This suggests that after the fast diffusion stage, the remaining CBM can also support the large amount of CBM desorbed in the transitional diffusion stage; however, it is insufficient for supporting more gas desorbed in the slow diffusion stage in the moderate-deformation degree of the coal seams.

Table 2 shows the amount of diffused CBM in the high-deformation degree of the coal seams in the fast diffusion stage (0.6–11.2 m^3/t, avg. = 7.2 m^3/t) dominates almost 70% of the total amount, which suggests that the desorbed CBM can diffuse more quickly in the fast diffusion stage and there are negligible limitations from the influences of the development of pores and fractures/cleats in the coal seam. After the fast diffusion stage, the remaining CBM cannot support a large amount of gas desorbed in the transitional diffusion stage (0.2–6.7 m^3/t, avg. = 2.3 m^3/t) and the slow diffusion stage

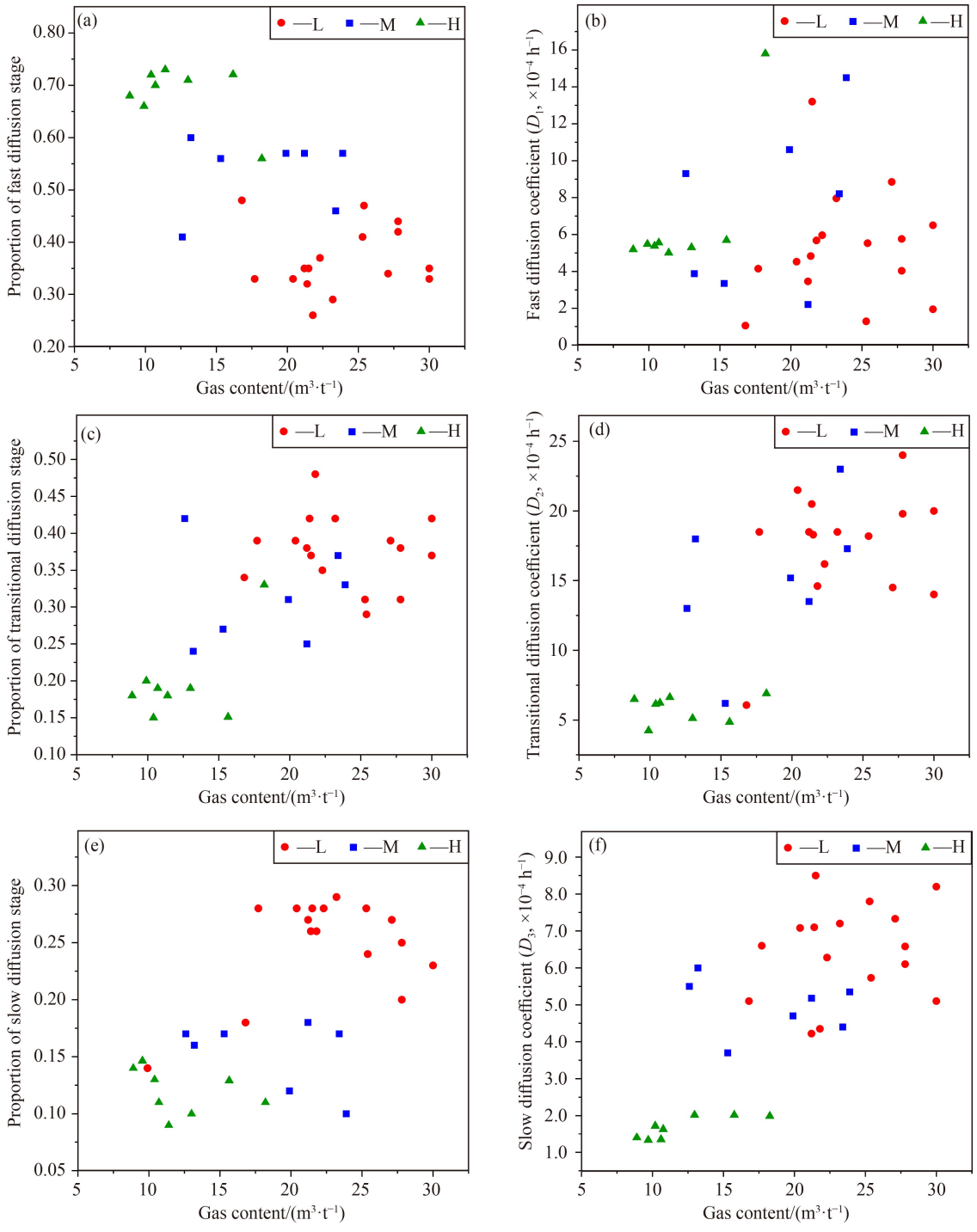

Fig. 6 The relationship between the proportion of fast diffusion stage and gas content (a), fast diffusion coefficient and gas content (b), the proportion of transitional diffusion stage and gas content (c), transitional diffusion coefficient and gas content (d), the proportion of slow diffusion stage and gas content (e) and slow diffusion coefficient and gas content (f), L,M and H respent low to high defor mation degree coal seams, respectively.

(0.1–2.2 m^3/t, avg. = 1.2 m^3/t), which reduces the rate of CBM diffusivity for these stages (Figs. 6(d) and 6(f)).

4.4 Effects of different diffusion stages on gas production rate

Figure 7 shows the production trend of five typical wells (P-ZS19, P-ZS11, P-ZS2, P-AS9, and P-AS2) that have been produced over 600 days. The CBM production rate of high-deformation degree of the coal seam rapidly reaches a peak (P-ZS2 = 95 days and P-AS2 = 50 days), followed by moderate-deformation degree coal seams (P-ZS11 = 130 days and P-AS9 = 135 days) and low-deformation degree coal seam (P-ZS19 = 210 days). P-

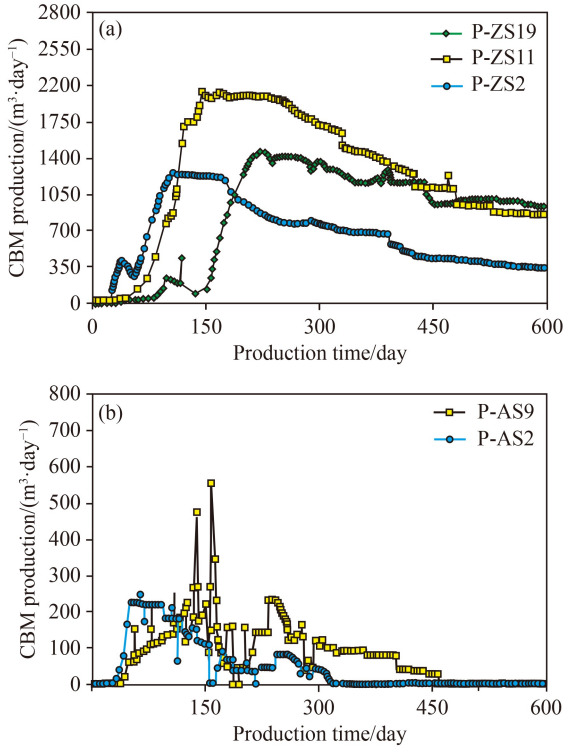

Fig. 7 The CBM production trend of five representative wells in the SQB. The location of these wells can be seen in Fig. 1.

ZS11 has the highest peak of CBM production rate (~2200 m^3/d) and stabilizes the peak production for ~100 days. The CBM production rate of P-ZS11 gradually decreases after ~230 days. Furthermore, the CBM production rate of P-ZS11 is finally close to ~900 m^3/d, which is noticeably higher than that of P-ZS2. The CBM production rates of P-AS9 and P-AS2 are generally low at < 600 m^3/day, rapidly decay after the peak production, and finally become 0 m^3/d after 320 to 460 days. These results suggest that coals with different deformation degree and gas content show the unique characteristics of the production of CBM per day, the time of peak production, and the stable production period of CBM wells. The behavior of CBM diffusion is related to the gas content and/or the deformation degree of the coal seam. Thus, it seems that the behavior of CBM diffusion can affect the characteristics of CBM production in the SQB.

5 Conclusions

The behavior of CBM diffusion demonstrates noticeable three-stage characteristics (i.e., fast, moderate, and slow diffusion stages), and the difference in the values between two adjacent diffusion stages is about an order of magnitude. This suggests that the multi-porous diffusion model can represent the behavior of CBM diffusion of the No. 3 coal seam in the SQB.

The regional distribution characteristics of CBM diffusion are different for different deformation degrees of the coal seams in the SQB. Considering the amount and rate of diffused CBM, the low deformation, moderate deformation and high deformation degrees of the coal seams present a relatively equitable distribution of three diffusion stages, a dominant role of the fast and transitional diffusion stages, and a dominant role of the fast diffusion stage, respectively.

The unique characteristics of gas diffusion are probably determined by a combined effect of the developed degree of pores as well as fractures/cleats and gas content in coal seams, causing a variation in the main production stage of the gas production history of the wells. Because gas content and the development degree of pores and fractures/cleats are closely associated with the deformation degree of the coal seams, differently deformed coal seams predict the unique characteristics of the production of CBM per day, the time to reach the peak production and the period of stable production. Thus, the behavior of gas diffusion has a strong correlation with the characteristics of gas production and can be used for predicting gas production potential.

Acknowledgment We acknowledge financial support from the National Natural Science Foundation of China (Grant Nos. 42125205, 41830427, and 42102227).

References

Cai Y D, Liu D M, Yao Y B, Li J Q, Qiu Y K (2011). Geological controls on prediction of coalbed methane of No. 3 coal seam in southern Qinshui Basin, north China. Int J Coal Geol, 88(2–3): 101–112

Charrière D, Pokryszka Z, Behra P (2010). Effect of pressure and temperature on diffusion of CO_2 and CH_4 into coal from the Lorraine Basin (France). Int J Coal Geol, 81(4): 373–380

Cheng Y P, Pan Z J (2020). Reservoir properties of Chinese tectonic coal: a review. Fuel, 260: 116350

Clarkson C R, Bustin R M (1999). The effect of pore structure and gas pressure upon the transport properties of coal: a laboratory and modeling study. 2. Adsorption rate modeling. Fuel, 78(11): 1345–1362

Clarkson C R, Salmachi A (2017). Rate-transient analysis of an undersaturated CBM reservoir in Australia: accounting for effective permeability changes above and below desorption pressure. J Nat Gas Sci Eng, 40: 51–60

Dong J, Cheng Y P, Pan Z J (2020). Comparison of transient and pseudo-steady diffusion of methane in coal and implications for coalbed methane control. J Petrol Sci Eng, 184: 106543

Jia Q F, Liu D M, Cai Y D, Fang X L, Li L G (2021). Petrophysics characteristics of coalbed methane reservoir: a comprehensive review. Front Earth Sci, 15(2): 202–223

Karacan C Ö, Ruiz F A, Cotè M, Phipps S (2011). Coal mine methane: a review of capture and utilization practices with benefits to mining safety and to greenhouse gas reduction. Int J Coal Geol, 86(2–3): 121–156

Keshavarz A, Sakurovs R, Grigore M, Sayyafzadeh M (2017). Effect of maceral composition and coal rank on gas diffusion in Australian coals. Int J Coal Geol, 173: 65–75

Li J Q, Lu S F, Zhang P F, Cai J C, Li W B, Wang S Y, Feng W J (2020). Estimation of gas-in-place content in coal and shale reservoirs: a process analysis method and its preliminary application. Fuel, 259: 116266

Li Z T, Liu D M, Cai Y D, Shi Y L (2016). Investigation of methane diffusion in low rank coals by a multiporous diffusion model. J Nat Gas Sci Eng, 33: 97–107

Li Z T, Liu D M, Wang Y J, Si G Y, Cai Y D, Wang Y P (2021). Evaluation of multistage characteristics for coalbed methane desorption-diffusion and their geological controls: a case study of the northern Gujiao Block of Qinshui Basin, China. J Petrol Sci Eng, 204: 108704

Liu D M, Yao Y B, Wang H (2022a). Structural compartmentalization and its relationships with gas accumulation and gas production in the Zhengzhuang Field, southern Qinshui Basin. Int J Coal Geol, 259: 104055

Liu D M, Qiu F, Liu N, Cai Y D, Guo Y L, Zhao B, Qiu Y K (2022b). Pore structure characterization and its significance for gas adsorption in coals: a comprehensive review. Unconv Resour, 2: 139–157

Liu D M, Yao Y B, Chang Y H (2022c). Measurement of adsorption phase densities with respect to different pressure: potential application for determination of free and adsorbed methane in coalbed methane reservoir. Chem Eng J, 446: 137103

Liu T, Lin B Q, Fu X H, Gao Y B, Kong J, Zhao Y, Song H R (2020). Experimental study on gas diffusion dynamics in fractured coal: a better understanding of gas migration in *in-situ* coal seam. Energy, 195: 117005

Lu S Q, Cheng Y P, Li W, Wang L (2015). Pore structure and its impact on CH_4 adsorption capability and diffusion characteristics of normal and deformed coals from Qinshui Basin. Int J Oil Gas Coal Technol, 10(1): 94–114

Meng Y, Li Z P (2016). Experimental study on diffusion property of methane gas in coal and its influencing factors. Fuel, 185: 219–228

Moore T A (2012). Coalbed methane: a review. Int J Coal Geol, 101: 36–81

Pan J N, Zhu H T, Hou Q L, Wang H C, Wang S (2015). Macromolecular and pore structures of Chinese tectonically deformed coal studied by atomic force microscopy. Fuel, 139: 94–101

Pillalamarry M, Harpalani S, Liu S M (2011). Gas diffusion behavior of coal and its impact on production from coalbed methane reservoirs. Int J Coal Geol, 86(4): 342–348

Staib G, Sakurovs R, Gray E M A (2015). Dispersive diffusion of gases in coals. Part I: model development. Fuel, 143: 612–619

Tang X, Li Z Q, Ripepi N, Louk A K, Wang Z F, Song D Y (2015). Temperature-dependent diffusion process of methane through dry crushed coal. J Nat Gas Sci Eng, 22: 609–617

Wang H, Yao Y B, Liu D M, Pan Z J, Yang Y H, Cai Y D (2016). Fault-sealing capability and its impact on coalbed methane distribution in the Zhengzhuang field, southern Qinshui Basin, north China. J Nat Gas Sci Eng, 28: 613–625

Wang H, Yao Y B, Liu D M, Cai Y D, Zhou S Q (2022). Determination of the degree of coal deformation and its effects on gas production in the southern Qinshui Basin, north China. J Petrol Sci Eng, 216: 1107464

Xu H, Tang D Z, Zhao J L, Li S, Tao S (2015). A new laboratory method for accurate measurement of the methane diffusion coefficient and its influencing factors in the coal matrix. Fuel, 158: 239–247

Yang R, Ma T R, Xu H, Liu W Q, Hu Y, Sang S (2019). A model of fully coupled two-phase flow and coal deformation under dynamic diffusion for coalbed methane extraction. J Nat Gas Sci Eng, 72: 103010

Zhang J Y, Liu D M, Cai Y D, Yao Y B, Ge X (2018). Carbon isotopic characteristics of CH_4 and its significance to the gas performance of coal reservoirs in the Zhengzhuang area, Southern Qinshui Basin, north China. J Nat Gas Sci Eng, 58: 135–151

Zhao J L, Tang D Z, Qin Y, Xu H, Liu Y L, Wu H Y (2018). Characteristics of methane (CH_4) diffusion in coal and its influencing factors in the Qinshui and Ordos Basins. Energy Fuel, 32: 1196–1205

Ziarani A S, Aguilera R, Clarkson C R (2011). Investigating the effect of sorption time on coalbed methane recovery through numerical simulation. Fuel, 90(7): 2428–2444